Synthesis of CuO Nanoparticles from Copper(II) Schiff Base Complex: Evaluation via Thermal Decomposition

Ali Mudher Abdulkareem Al-Khazraji[1*], Enass Jasim Waheed[1], and Awf Abdul Rahman Ahmed[2]

[1]*Department of Chemistry, College of Education for Pure Science (Ibn Al-Haitham), University of Baghdad, Rusafa, Educational Complex, Al-Tayaran Square 42, Baghdad 10001, Iraq*

[2]*Ministry of Education, Directorate of Education, Rusaafa first, Baghdad – Rusafa, Street 52, Baghdad, 10001, Iraq*

* ***Corresponding author:***

tel: +964-7724031983
email: ali.m.ak@ihcoedu.uobaghdad.edu.iq

Received: April 4, 2024
Accepted: December 23, 2024

DOI: 10.22146/ijc.95427

Abstract: *Copper oxide (CuO) nanoparticles were synthesized through the thermal decomposition of a copper(II) Schiff-base complex. The complex was formed by reacting cupric acetate with a Schiff base in a 2:1 metal-to-ligand ratio. The Schiff base itself was synthesized via the condensation of benzidine and 2-hydroxybenzaldehyde in the presence of glacial acetic acid. This newly synthesized symmetric Schiff base served as the ligand for the Cu(II) metal ion complex. The ligand and its complex were characterized using several spectroscopic methods, including FTIR, UV-vis, ^{1}H-NMR, ^{13}C-NMR, CHNS, and AAS, along with TGA, molar conductivity and magnetic susceptibility measurements. The CuO nanoparticles were produced by thermally decomposing the complex at 800 °C. These nanoparticles and other metal oxides are highly valued in various industries for their optical, magnetic, and electrical properties. The experiment highlighted the synthesis of CuO nanoparticles through the thermal breakdown of copper(II) ions, starting with copper acetate, which reacted with the ligand to form the complex. The characterization results of CuO nanoparticles reveal a highly pure crystalline structure with an average size of 70–90 nm.*

Keywords: *benzidine; copper(II) Schiff-base complex; CuO nanoparticles; energy gap; nanoparticles*

■ INTRODUCTION

Schiff bases are chemical compounds characterized by the presence of the azo-methine group (C=N) [1-2]. They are typically formed by the reaction of carbonyl groups with primary amines. These compounds are known for their ability to function as ligands, forming metal complexes that stabilize metal ions in various oxidation states. Their unique properties make them essential in a range of catalytic and industrial processes.

Metal complexes of Schiff bases that contain oxygen and nitrogen as donor atoms are particularly noteworthy due to their flexibility, sensitivity to environmental changes, and distinctive structural characteristics. Copper-binding Schiff-base ligands, in particular, have gained significant attention for their applications in optoelectronics, catalysis, and biomolecular studies [3]. Previous research has explored the synthesis of various Schiff bases through condensation processes [4]. Among these, the complexes derived from benzidine and benzaldehyde, have been investigated. These complexes are of interest not only for their coordination properties but also for their potential in catalysis and other functional applications.

Nanoparticles have emerged as a significant area of interest due to their diverse applications, including photocatalysis. Copper(II) oxide (CuO) nanoparticles are especially noteworthy, finding use in photocatalytic processes, dye-sensitized solar cells, gas sensors, thermoelectric devices, and more. CuO nanoparticles can be synthesized in various forms, such as rods, nanoplates, and tubes, using techniques like chemical precipitation, sol-gel methods, electrochemical synthesis, microwave-assisted thermal processes, and

green synthesis. The thermochemical breakdown [5] of copper(II) complexes has also been extensively studied to produce CuO nanoparticles. The synthesis of CuO nanoparticles is effective, straightforward, and often solvent-free, as demonstrated by several studies [6].

The current research employs advanced characterization techniques, including ^{1}H- and ^{13}C-NMR, UV-vis, and FTIR spectroscopy, to analyze the molecular structure of these compounds. Additionally, combustion synthesis (illustrated in Scheme 1) was utilized to produce CuO nanoparticles. The shape and structure of the nanoparticles were examined using X-ray diffraction (XRD), scanning electron microscopy (SEM), energy dispersive X-ray spectroscopy (EDX), transmission electron microscopy (TEM), and Brunauer-Emmett-Teller (BET) analysis.

The use of copper-Schiff base complexes offers a practical and efficient method for synthesizing CuO nanoparticles. This approach allows for better control over the size and morphology of the nanoparticles while requiring milder reaction conditions and producing higher-purity products. Furthermore, Schiff base ligands provide the versatility needed to modify nanoparticle properties, such as surface chemistry and catalytic activity, enabling the development of multifunctional materials. The simplicity of this synthesis method, combined with the potential use of naturally occurring ligands, makes it an environmentally friendly and scalable approach. However, the success of this method depends on the choice of specific Schiff base ligands and reaction conditions.

■ EXPERIMENTAL SECTION

Materials

The benzidine, absolute ethanol, 2-hydroxybenzaldehyde, diethyl ether, acetic acid, and ($Cu(CH_3COO)_2$ were used in this experiment (99%, Merck, Germany). The materials remained used without purification.

Instrumentation

The UV-vis spectra of the synthesized compounds were measured using a SHIMADZU UV-1800 spectrophotometer in the range of 300–800 nm. FTIR spectra were recorded with a SHIMADZU 8400 FTIR spectrophotometer, utilizing KBr discs for analysis within the 400–4000 cm^{-1} range. Electrical conductivity measurements were performed using a WTW conductivity meter in DMF solutions (1×10^{-3} C) at 25 °C in the Chemistry Department of Al-Mustansiriya University. Thermal analysis of both the ligand and the complex was conducted using a STA TT-1000 thermogravimetric analyzer (Japan, Jordan). NMR spectra of the synthesized compounds were recorded on a BRUKER AV 400 Avance-III (500 MHz and 125 MHz) instrument at the National Institute of Technology in Tehran, Iran, with DMSO-d_6 as the solvent and TMS as the internal standard. The morphology of CuO nanoparticles was observed using a TEM (model 912A-B, Germany) at the University of Tehran and an SEM (MIRA3, TESCAN, Czech) at the Institute of Technology, Jordan. XRD analysis was performed using a Bruker 2D Phaser X-ray Diffractometer (Germany) at the Central Organization for Standardization and Quality Control (COSQC). The surface area of the samples was analyzed using a BET surface area analyzer (AIS-2300, Japan, Jordan). Metal content was measured using atomic absorption spectroscopy (AAS) with a Nova 350 spectrophotometer at the Ibn Sina State Company.

Procedure

Synthesized of 2,2'-((1E,1'E)-([1,1'-biphenyl]-4,4'diylbis(azaneylylidene))bis(methaneylylidene))diphenol ligand and its complex

In a 250 mL round-bottom flask, benzidine (0.082 mmol, 4.8 g) and 2-hydroxybenzaldehyde (0.076 mol, 25 mL) were blended and dissolved using the condensation method (see Scheme 1) in 35 mL of ethanol, along with four drops of glacial-ethanoic acid. The mixture was refluxed and heated for 8 h. Afterward, the resulting precipitate was filtered, dried, and recrystallized under reduced pressure for purification. The compound solidified after the solvent was removed under low pressure. An ethanol solution was used to recrystallize it, with a melting point of 173–176 °C [6]. The product was named Schiff base ligand (L). To prepare the chelation complex, an aqueous solution of

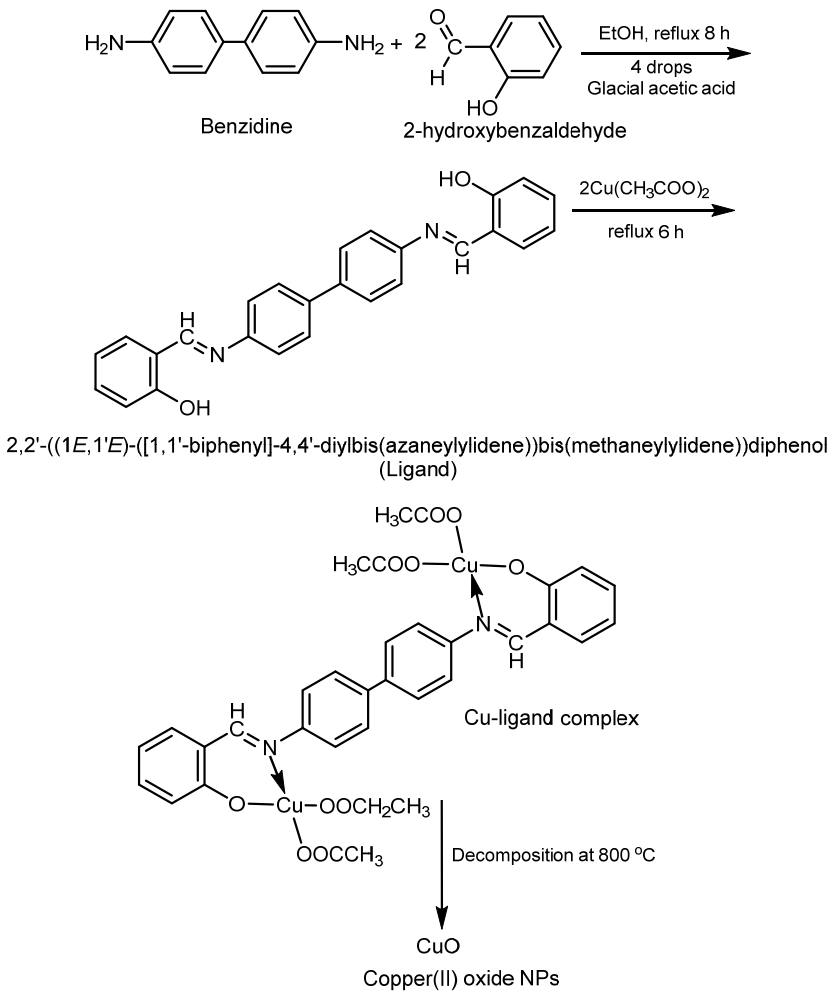

Scheme 1. Synthesis ligand Schiff base, copper complex, and CuO nanoparticles

the copper acetate ($Cu(CH_3COO)_2$) (4 g, 0.042 mol) was mixed with an ethanolic solution of the ligand (3 g, 0.018 mol) in a 2:1 (M:L) ratio, as illustrated in Scheme 1. The mixture was refluxed at 110 °C and stirred for 6 h. A white solid precipitate formed from the heated ethanol, with a melting point of 195–202 °C. After cooling to room temperature, the solid was filtered, dried, and recrystallized [7].

Synthesis CuO nanoparticle

CuO nanoparticles were synthesized by heating the white powders of a Cu-Schiff base complex. Approximately 1.2 g of the powder was placed in a platinum crucible, which was then positioned in an electric furnace. In the presence of air, the powder was heated at 10 °C/min, with the temperature gradually increasing to 800 °C over 3 h. As shown in Scheme 1, the resulting CuO nanoparticles were washed with ethanol and air-dried [8].

■ RESULTS AND DISCUSSION

FTIR Spectra of Ligand and Its Copper Complex

The presence of ligand was confirmed by the identification in Fig. 1 of a new vibration band at 1658 cm^{-1} associated with the ν(C=N) imine group. Other bands at 1405 and 3067 cm^{-1} were ascribed to the ν(C=C) str. and ν(C–H aromatic) str., respectively. The FTIR analysis of the copper complex was conducted using a potassium bromide disc. The stretching frequency of the ν(C=N) group [9] at 1658 cm^{-1} for the free ligand (L) was relocated to 1642 cm^{-1} due to the engagement of the imine group in coordination with the metal. In the spectrum of the complex, it was observed that the band of

the phenolic group present at 3144 cm^{-1} in the spectrum of the ligand vanished with the carbonyl band shifted to longer wavelengths. All data is included in Table 1.

^{1}H- and ^{13}C-NMR for Ligand

Fig. 2(a) illustrates the ^{1}H-NMR spectrum of the ligand subsequent to its is dissolved in DMSO-d_6. The observation of the proton of L occurred as a single peak (singlet) at 7.9 ppm (1H) and had a chemical shift of CH=N. The aromatic protons in the central benzene ring showed chemical shifts of 7.3 ppm (m, 8H, Ar-H), while the terminal benzene ring had chemical shifts of 5.9 ppm (m, 4H, Ar-H). The hydroxyl proton appeared as a singlet at 10.85 ppm (2H), indicating a significant peak. Consequently, the ^{13}C-NMR spectra of the Schiff base ligand are presented in Fig. 2(b). One of the important qualities is the existence of two azomethine group (N=CH) [10], which had a peak at 160.9 ppm. The C-atom from the OH group was located at 161 ppm. For aromatic compounds, the C-atoms within the linkage of the two central benzene rings shifted at 138 ppm, while the benzene ring terminal shifted at 132.6 ppm. Finally, the amine group's carbon shifted at 151 ppm.

UV-vis of Schiff-base Ligand and Its Copper Complex

Table 2 and Fig. 3 demonstrate the compound L's UV-vis absorption spectrum in the TMF solution. The electronic spectra were identified in 2 bands at 368 and 562 nm, corresponding to 27173 and 17793 cm^{-1} complex in TMF solution exhibited 3 bands at 371, 527,

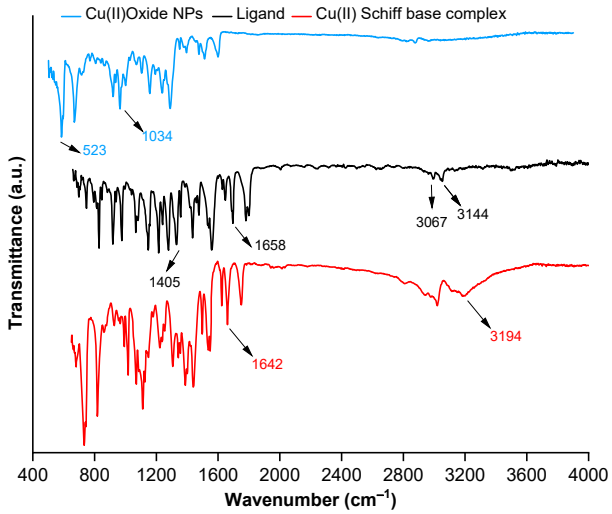

Fig 1. FTIR spectra for Cu(II) oxide NPs, Schiff base, and Cu(II) Schiff base complex

Table 1. FTIR data for CuO NPs, Schiff base (L), and copper complex

Band	Wavenumber (cm^{-1})		
	Schiff base (L)	Cu(II) Schiff base complex	CuO
ν(O–H) alcohol intramolecular bonded	3144	3194	-
ν(C=N) str. imine group	1658	1642	-
ν(C=C) str. aromatic	1405	-	-
ν(C–H) str. aromatic	3067	-	-
ν(C–O)	1086	1069	-
ν(Cu–O)	-	-	523

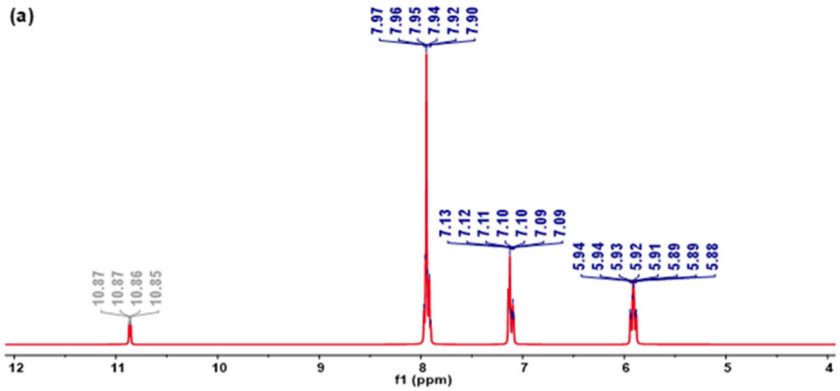

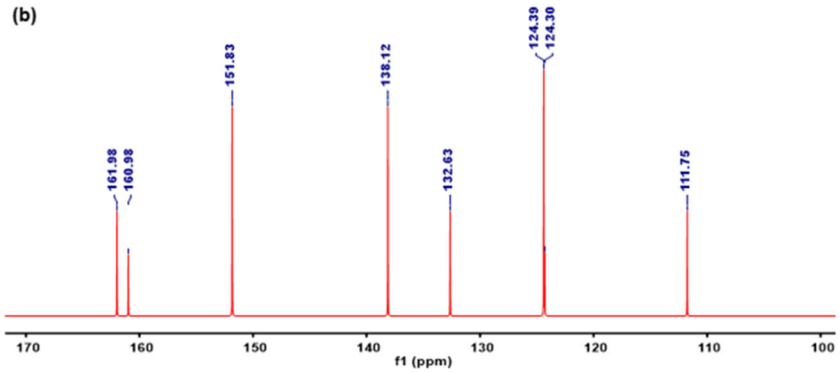

Fig 2. (a) ^{1}H-NMR and (b) ^{13}C-NMR spectra for Schiff base (L)

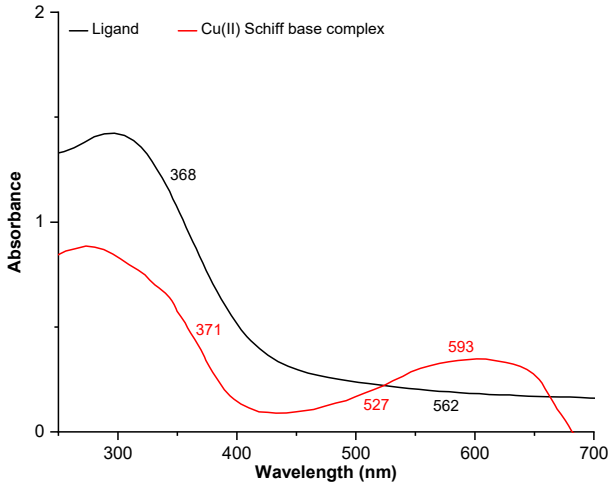

Fig 3. UV-vis of the copper complex and ligand Schiff-base

Table 2. UV-vis of copper complex and ligand Schiff-base

Comp.	λ_{max}, nm (ν, cm^{-1})	Transitions	Suggested structure
Ligand Schiff base	368 (27,173)	n–π*	-
	562 (17,793)	π–π*	
CuL	371 (26,954)	n–π*	Tetrahedral
	527 (18,975)	π–π*	
	593 (16,863)	Cu→LCT	

and 593 nm, corresponding to wavelengths 26954, 18975, and 16863 cm^{-1}, respectively. These bands are associated with the n-π*, π-π*, and Cu→LCT transitions within a tetrahedral geometry.

TGA and DTA Thermal Analysis of the Schiff-base Ligand and Its Copper Complex

The TG and DTA trends of the metal ion complexes and the ligand Schiff base under N_2 gas, heat-up at a rate of 10 °C/min, are displayed in Fig. 4. The first step, which is endothermic, occurs at temperatures ranging from 80 to 110 °C and is due to the loss of two water molecules and four acetate molecules. The second exothermic process occurs between 280 and 325 °C and is caused through the removal of two six-ring (benzene) terminals [11]. The third exo-thermic step takes place within the temperature range of 440 to 510 °C and is a result of the breaking up of segment residue organic varieties reduction. Finally, there is an exothermic process of metal copper oxidation, resulting in the formation of CuO, which occurs at temperatures between 630 and 780 °C.

Characterization of CuO Nanoparticle

A typical complex was heated at 780 °C for 4 h to produce CuO nanoparticles. The resulting CuO was examined using various techniques, including UV-vis

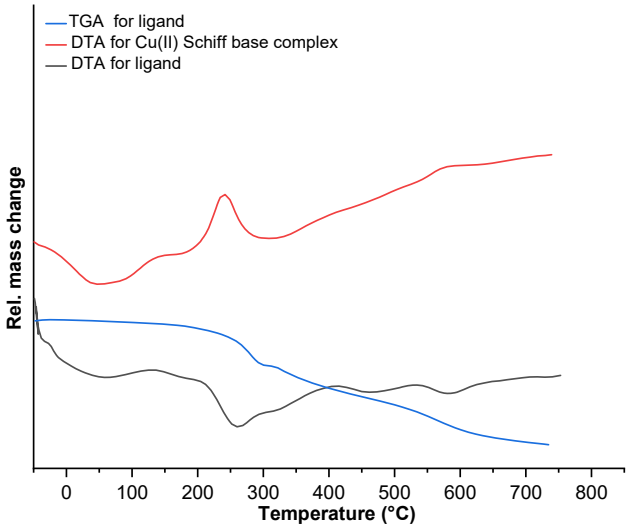

Fig 4. TGA and DTA investigation of the copper complex and Schiff base ligand

diffuse reflectance, BET pattern analysis, FTIR, XRD, TEM, SEM, and EDX to determine its properties.

The CuO nanostructure's FTIR

Fig. 1 indicates the results of the FTIR analysis on the CuO NPs, which encompassed a range of 4000 to 400 cm^{-1}. The CuO NPs consist of (Cu–O) bonds, as demonstrated by the absorption peaks at 523 cm^{-1}. It is apparent from the observed FTIR spectra indicate that the synthesis of CuO NPs was adequate [8].

UV-vis diffuse reflectance for CuO NPs

CuO NPs are of significance to sectors, including optoelectronics and catalysis, due to their distinctive electrical and optical characteristics. By using UV diffuse reflectance spectroscopy, one may effectively investigate the material's band structure. We determine the optical bandgap of CuO NPs via the frequently employed Tauc technique, which can be utilized to estimate the energy gap in semiconductors. The explicit bandgap energy E_g in Fig. 5 was calculated by implementing reflection to the CuO NPs' immediate transition Eq. (1) [12];

$$(\alpha h\nu)^{\gamma} = A\left(h\nu - E_g\right)^{n} \quad (1)$$

The absorption coefficient is represented by the symbol α, photon energy by hν, and the optical bandgap by E_g. A is a constant, and n is the Tauc exponent. The direct band gap is determined to be 2.38 eV by graphing $(h\nu)^2$ versus photon energy and extending the linear portion of the curve until absorption becomes zero.

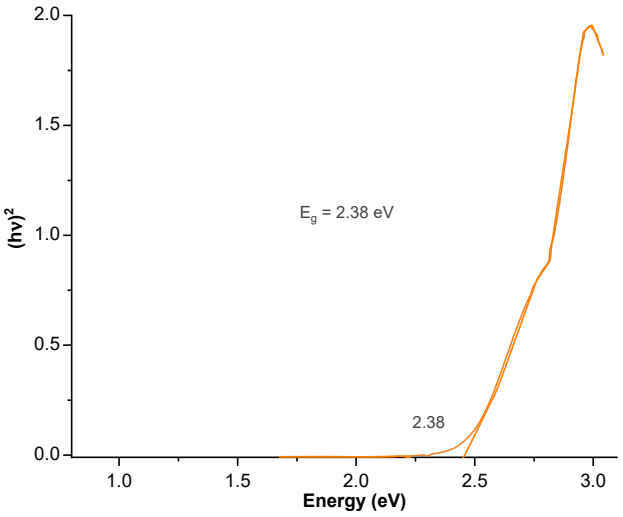

Fig 5. Energy bandgap for CuO NPs

XRD analysis of CuO NPs

The X-ray beam is the basic method for determining the size of crystals and solid crystalline structures, which in turn hits the sample and, in accordance with Bragg's rule, is dispersed by the crystal phases [13], as shown in Eq. (2);

$$n\lambda = 2d\sin\theta \quad (2)$$

where the incident X-ray beam's wavelength is represented by λ, the reflection order is represented by n. Then, d is the distance between crystal lattice planes. The X-ray beam's incidence angle is symbolized as θ.

The properties that hold utmost significance in a diffraction pattern are peak position, shape and intensity, which can be acquired by figuring out each unit cell's Miller indices (h k l) and then comparing the peak positions to the standard patterns established by the material's structure. Furthermore, by utilizing Sherrer's formula [14], as shown in Eq. (3). The XRD data can also provide insights into the size of the crystallite.

$$D = \frac{K\lambda}{\beta\cos\theta} \quad (3)$$

The average crystallite size, denoted as L, is related to the shape factor (typically a constant around 0.9). The wavelength of the X-rays or neutrons indicated as λ (1.5406 Å), is also essential. B represents the full width at half maximum (FWHM) [15] of the diffraction peak, and θ is the Bragg's angle. In Fig. 6, the XRD data for

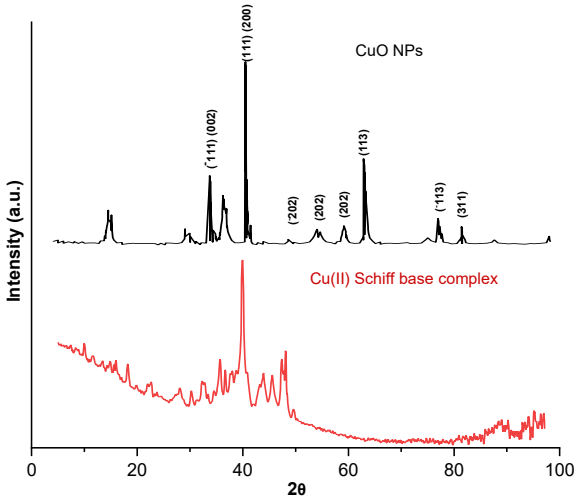

Fig 6. XRD for Cu(II) Schiff base complex and copper(II) oxide nanoparticles

CuO NPs is compared to the standard reference for CuO. The peaks found in the diffraction analysis, specifically (100), (002), (101), (102), (110), (103), and (112), were in line with the hexagonal CuO (wurtzite) [16] pattern from the standard reference. Fig. 6. clearly shows three distinct peaks for copper oxide at angles 35.9°, 38.5°, 39.6°, and 48.1° compared to the database of the Joint Committee on Powder Diffraction Standards (JCPDS).

SEM and EDX analysis for synthesized CuO

In Fig. 7, CuO NPs heated to 700 °C were examined for morphology and structure utilizing SEM techniques. The investigation revealed that the nanoparticles were not uniformly distributed and lacked a perfectly spherical form. According to the histogram statistics, the average size ranged from 60–71.2 nm [17-18]. Using EDX analysis, the production of CuO NPs was studied, and various regions were identified during the analysis. In Fig. 8, the peaks obtained from the analysis are shown. CuO in the produced nanostructure was confirmed by EDX spectroscopy, with atomic percent values of 60.84% for Cu and 39.16% for O. Although the synthesized samples contained Cu and O dopants, no significant impurities were found [17,19].

TEM of CuO nanoparticles

Fig. 9 depicts TEM images of CuO. This photograph was obtained to assist in comprehending the crystal characteristics and nanoparticle size. The TEM image indicates that the CuO particles have a nearly hexagonal form with slightly varying thicknesses. This verifies the SEM results, which showed that surface data from TEM may be used to investigate the surface of CuO NPs [20].

Surface area analyzer

The BET method is well-established to measure an available surface specific area by studying the physical adsorption of gas on solid surfaces. The adsorption isotherm, which plots the amount of gas that has been adsorbed onto the surface area against the relative pressure (P/P_0) at a constant temperature can be interpreted by this analysis. The BET analysis generally gives a Type II or Type IV isotherm, which depends on the pore structure present in the material. Isotherm-Specific Surface Area Correlation: The surface area relates

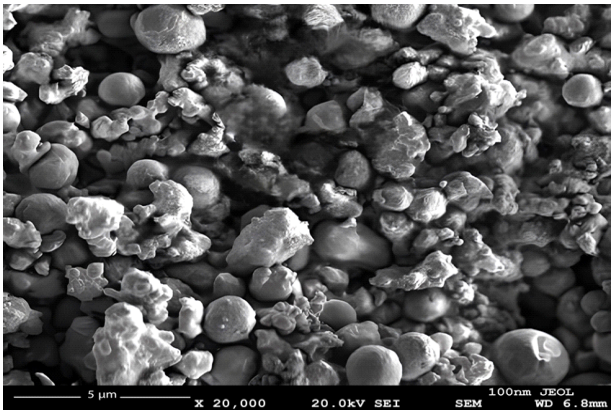

Fig 7. SEM analysis of CuO NPs

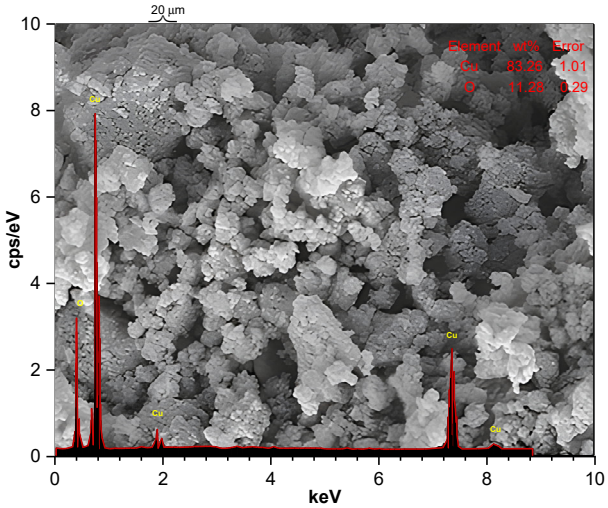

Fig 8. EDX analysis of CuO NPs

Fig 9. TEM image of CuO NPs

directly to the quantity of gas adsorbed in the monolayer. The BET equation takes the isotherm data (or at least the linear part of a BET plot) and calculates monolayer capacity in absolute normal liquid pressure. Fig. 10 illustrates the nitrogen isothermal adsorption technique for evaluating CuO NPs' pore structure and surface area. The CuO isotherm profiles indicated a minor hysteresis loop. Table 3 illustrates the CuO NPs' aggregate pore volume, average pore diameter, and

surface area. It is speculated that the CuO NPs' high surface energy leads them to aggregate or create bigger particles. The BET investigation deals with the adsorption of nitrogen.

According to the BET measurement, CuO NPs have a specific surface area. Eq. (4) is implemented to determine the effective diameter of the BET. A method was applied to determine CuO NPs' specific surface area (As) [4]. Before conducting the analysis, the material underwent a degassing process at a temperature of 140 °C for a duration of 4 h.

$$d_{BET} = \frac{6}{\rho As} \quad (4)$$

The particle density (ρ) of the CuO powder was 6.71 g/cm^3. The principal particle size (d_{BET}) and specific surface area (As) are specified. The passage reports that CuO NPs that were annealed at 780 °C acquired a mean crystallographic size of 8.61 nm via Eq. (4). The variation relates to the XRD Scherrer formula and the BET techniques [21] to determine the CuO NPs' average crystalline size. This disparity implies the presence of CuO NP clusters.

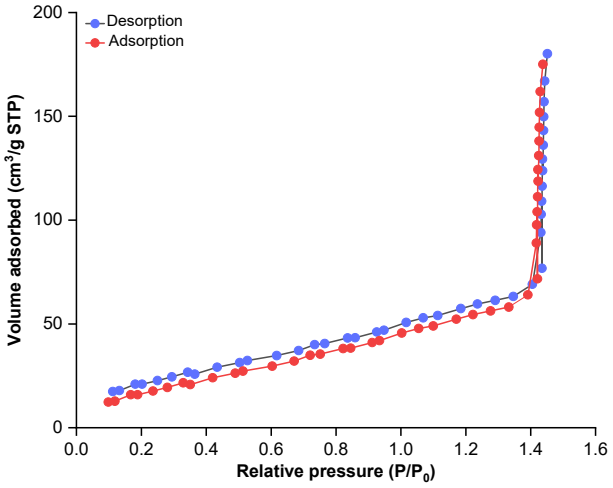

Fig 10. CuO adsorption-desorption isotherms utilizing BET surface analysis and N_2 gas

Table 3. Physical surface data for CuO

Physical parameters of a surface	Value
Surface of area	660.8 m^2/g
Average pore diameter	31.23 cm^3/g (STP)
Total pore volume	0.216 cm^3/g

CONCLUSION

Benzidine, 2-hydroxybenzaldehyde, and copper(II) acetate were combined to form a copper Schiff-base complex. The compound's structure was examined using a variety of analytical techniques, including FTIR, DTA, ^{1}H-NMR, ^{13}C-NMR, TGA, and UV-vis characterization. Although the Schiff base ligand to metal ratio was determined to be 1:2, the results demonstrated that the complex might comprise distorted tetrahedral molecular structures. Furthermore, the Cu-Schiff base combination was thermally broken down to produce CuO NPs. The energy band gap of these nanoparticles was 2.38 eV, and the particle size was 81 nm. Characterizations using XRD, EDX, SEM, TEM, and BET studies were performed to validate the production of CuO NPs. The findings showed the presence of single-phase CuO NPs with sizes smaller than 100 nm. These findings have significant implications for anticipating the behavior of CuO NPs. They could be utilized as a starting point for *in vitro* research in the future. The CuO NPs may also be utilized to create photocatalytic processes for the degradation of organic contaminants in water and the atmosphere. Although CuO is a semiconductor, it is beneficial for trapping light energy for catalytic processes. Overall, this work provides valuable information on the synthesis and characterization of CuO NPs and their wide applications.

ACKNOWLEDGMENTS

We would like to express our heartfelt gratitude to the Universities of Baghdad and Al-Mustansiriya personnel for their technical support and help throughout the study.

CONFLICT OF INTEREST

We confirm the absence of any conflict of interest.

AUTHOR CONTRIBUTIONS

Ali Mudher Abdulkareem Al-Khazraji, Enass Jasim Waheed, and Awf Abdul Rahman Ahmed were in charge of conceptualizing and designing the experiments, conducting the experiments, analyzing the data, writing the paper, providing financing, and

revising the paper. The authors actively participated in the discussion of the findings and provided substantial enhancements to the final written content.

■ REFERENCES

[1] Al-Khazraji, A.M.A., 2023, Synthesis of Co(II), Ni(II), Cu(II), Pd(II), and Pt(IV) complexes with 1^4,1^5,3^4,3^5-tetrahydro-1^1H,3^1H-4,8-diaza-1,3(3,4)-ditriazola-2,6(1,4)-dibenzenacyclooctaphane-4,7-dien-15,35-dithione, and the thermal stability of polyvinyl chloride modified complexes, *Indones. J. Chem.*, 23 (3), 754–769.

[2] Al-Daffaay, R.K.H., 2022, Preparation-and spectroscopic characterization of transition metal complexes with Schiff base 2-[1-(1*H*-indol-3-yl)ethylimino)methyl]naphthalene-1-ol, *Baghdad Sci. J.*, 19 (5), 1036–1044.

[3] Al-Redha, H.M.A., Ali, S.H., and Mohammed, S.S., 2022, Syntheses, structures and biological activity of some Schiff base metal complexes, *Baghdad Sci. J.*, 19 (3), 704–715.

[4] Alothman, A.A., and Albaqami, M.D., 2020, Nano-sized Cu(II) and Zn(II) complexes and their use as a precursor for synthesis of CuO and ZnO nanoparticles: A study on their sonochemical synthesis, characterization, and DNA-binding/cleavage, anticancer, and antimicrobial activities, *Appl. Organomet. Chem.*, 34 (10), e5827.

[5] Paul, S., Gogoi, H.P., Singh, A., and Barman, P., 2023, Nanostructured metal oxides by facile thermal decomposition of Zinc(II) and Copper(II) Schiff base complexes: Microwave synthesis of complexes, characterization, DFT study, optical properties and application of its oxides in multicomponent Biginelli reaction, *Inorg. Chem. Commun.*, 153, 110760.

[6] Al-Khazraji, A.M.A., Al Hassani, R.A.M., and Ahmed, A., 2020, Studies on the photostability of polystyrene films with new metals complex of 1,2,4-triazole-3-thione derivate, *Sys. Rev. Pharm.*, 11 (5), 525–534.

[7] Mahmood, W.A.R., Aldabbagh, A.K.A., and Mahmoud, M.A., 2022, Synthesis and characterization of new benzothiazole-derived Schiff bases metal complexes, *Baghdad Sci. J.*, 19 (2), 378–384.

[8] Parekh, Z.R., Chaki, S.H., Hirpara, A.B., Patel, G.H., Kannaujiya, R.M., Khimani, A.J., and Deshpande, M., 2021, CuO nanoparticles–synthesis by wet precipitation technique and its characterization, *Phys. B*, 610, 412950.

[9] Mahmood, T.S., Numan, A.T., and Waheed, E.J., 2020, Synthesis, spectroscopic identification and antimicrobial activity of mixed ligand complexes of new ligand [3-((4-acetyl phenyl)amino)-5,5-dimethylcyclohex-2-en-1-one](Hl*) with 3-amino phenol, *Biochem. Cell. Arch.*, 20 (1), 2235–2245.

[10] Abdulrahman, W.A., Othman, I.A., and Waheed, E.J., 2021, Metal complexes of ligand derived from amine compound: Formation, spectral characterization, and biological evaluation, *Int. J. Drug Delivery Technol.*, 11 (3), 728–734.

[11] Mahmoud, N.F., Abbas, A.A., and Mohamed, G.G., 2021, Synthesis, characterization, antimicrobial, and MOE evaluation of nano 1,2,4-triazole-based Schiff base ligand with some d-block metal ions, *Appl. Organomet. Chem.*, 35 (6), e6219.

[12] Fakhriza, M.A., Rusdiarso, B., Sunarintyas, S., and Nuryono, N., 2023, The addition of copper nanoparticles to mineral trioxide aggregate for improving the physical and antibacterial properties, *Indones. J. Chem.*, 23 (3), 692–701.

[13] Sagadevan, S., Vennila, S., Marlinda, A.R., Al-Douri, Y., Johan, M.R., and Anita Lett, J., 2019, Synthesis and evaluation of the structural, optical, and antibacterial properties of copper oxide nanoparticles, *Appl. Phys. A*, 125 (8), 489.

[14] George, A., Raj, D.M.A., Raj, A.D., Irudayaraj, A.A., Arumugam, J., Prabu, H.J., Sundaram, S.J., Al-Dhabi, N.A., Arasu, M.V., Maaza, M., and Kaviyarasu, K., 2020, Temperature effect on CuO nanoparticles: Antimicrobial activity towards bacterial strains, *Surf. Interfaces*, 21, 100761.

[15] Bin Mobarak, M., Hossain, M.S., Chowdhury, F., and Ahmed, S., 2022, Synthesis and characterization of CuO nanoparticles utilizing waste fish scale and exploitation of XRD peak

profile analysis for approximating the structural parameters, *Arabian J. Chem.*, 15 (10), 104117.

[16] Mansoor Al-Saeedi, A.M., Mohamad, F.K., and Ridha, N.J., 2022, Synthesis and characterization CuO-ZnO binary nanoparticles, *J. Nanostruct.*, 12 (3), 686–696.

[17] Radhakrishnan, A.A., and Beena, B.B., 2014, Structural and optical absorption analysis of CuO nanoparticles, *Indian J. Adv. Chem. Sci.*, 2 (2), 158–161.

[18] Batool, M., Qureshi, M.Z., Hashmi, F., Mehboob, N., and Shah, A.S., 2019, Congo red azo dye removal and study of its kinetics by aloe vera mediated copper oxide nanoparticles, *Indones. J. Chem.*, 19 (3), 626–637.

[19] Sahai, A., Goswami, N., Kaushik, S.D., and Tripathi, S., 2016, $Cu/Cu_2O/CuO$ nanoparticles: Novel synthesis by exploding wire technique and extensive characterization, *Appl. Surf. Sci.*, 390, 974–983.

[20] Waris, A., Din, M., Ali, A., Ali, M., Afridi, S., Baset, A., and Ullah Khan, A., 2021, A comprehensive review of green synthesis of copper oxide nanoparticles and their diverse biomedical applications, *Inorg. Chem. Commun.*, 123, 108–369.

[21] Geetha, M.P., Pratheeksha, P., and Subrahmanya, B.K., 2020, Development of functionalized CuO nanoparticles for enhancing the adsorption of methylene blue dye, *Cogent Eng.*, 7 (1), 1783102.